Electronic structure of LaO based on frozen-core four-component relativistic multiconfigurational quasidegenerate perturbation theory

Hiroko Moriyama,[1] Yoshihiro Watanabe,[2] Haruyuki Nakano,[2,3] Shigeyoshi Yamamoto,[4] and Hiroshi Tatewaki[1,a)]

[1]*Graduate School of Natural Sciences, Nagoya City University, Nagoya, Aichi 467-8501, Japan*
[2]*Department of Chemistry, Faculty of Sciences, Kyushu University, Fukuoka 812-8581, Japan*
[3]*CREST, Japan Science and Technology Agency (JST), Kawaguchi, Saitama 332-0012, Japan*
[4]*School of International Liberal Studies, Chukyo University, Nagoya, Aichi 466-8666, Japan*

(Received 21 November 2009; accepted 22 February 2010; published online 31 March 2010)

The electronic structure of the LaO molecule is studied using frozen-core four-component multiconfigurational quasidegenerate perturbation theory. The ground state and nine experimentally observed excited states are examined. The ground state is $^2\Sigma^+_{1/2}$ and its gross atomic orbital population is La($5p^{5.76}6s^{0.83}6p^{0.14}p^{*0.21}d^{*1.17}f^{*0.26}$) O($2p^{4.63}$), where p^*, d^*, and f^* are the polarization functions of La that form molecular spinors with O $2ps$. We found that it is not necessary to consider the excitation from the O $2p$ electrons when analyzing the experimental spectra. This validates the foundation of the ligand field theory on diatomic molecules, including the La atom where only one electron is considered. The spectroscopic constants R_e, ω_e, and T_0 calculated for the ground state and low-lying excited states $A'(^2\Delta_{3/2})$, $A'(^2\Delta_{5/2})$ $A(^2\Pi_{1/2})$, and $A(^2\Pi_{3/2})$ are in good agreement with the experimental values. © *2010 American Institute of Physics*. [doi:10.1063/1.3359854]

I. INTRODUCTION

The LaO molecule has long been known to play an important role in cool stellar atmosphere; the absorption spectra of red ($A \rightarrow X$) and yellow-green ($B \rightarrow X$) are prominent in some S-type stars which have a low surface temperature, around 3300 K.[1–3] Furthermore there exist many molecules, including the superconductor $La_{2-x}Sr_xCuO_4$,[4] in which the characteristics of the bonds are little known. Since LaO is the simplest lanthanide monoxide, it is important to investigate the LaO molecule as a foundation for discussing the electronic structure of larger lanthanide compounds.

Experimental and theoretical assignments are summarized in Table I. Experimental studies of LaO have been collected by Huber and Herzberg[5] and Carette.[2] The ground state of LaO was originally assigned as $^4\Sigma^+$. Berg *et al.*[6] questioned this assignment, and Weltner *et al.*[7] asserted that the ground state was $^2\Sigma^+$. For the excited states of this molecule, six spectrum systems are by now well known. They are red ($A\ ^2\Pi_{1/2\ or\ 3/2} \rightarrow X\ ^2\Sigma^+$), orange ($C\ ^2\Pi_{1/2\ or\ 3/2} \rightarrow A'\ ^2\Delta_{3/2or\ 5/2}$), yellow-green ($B\ ^2\Sigma^+ \rightarrow X\ ^2\Sigma^+$), blue ($C\ ^2\Pi_{1/2\ or\ 3/2} \rightarrow X\ ^2\Sigma^+$), and violet systems ($D\ ^2\Sigma^+ \rightarrow X\ ^2\Sigma^+$, $F\ ^2\Sigma^+ \rightarrow X\ ^2\Sigma^+$). Several theoretical studies exist, such as the ligand field theory (LFT) model calculations of Carette.[2] Kaledin *et al.*[8] proposed that A′, A, and B have $5d^1$ configurations while C and D are $6p^1$, as shown in Table I. Schamps *et al.*[9] studied the electronic structures of LaO by comparing LFT and a multireference configuration interaction (MRCI) calculation under the *LS* coupling scheme. Their assignments for the lowest six states are the same as those of Kaledin *et al.* Kotzian *et al.*[10] performed semiempirical calculations, based on the intermediate neglect of differential overlap (INDO) technique for lanthanide monoxides. Their assignments for A′, A, B, C, and D are $5d^1$, $6p^1$, $6p^1$, $4f^1$, and $4f^1$, respectively. These are different from those of Kaledin *et al.* and Schamps *et al.* Carette[2] gives another assignment. The calculated excitation energies generally agree with those of experiment, although the respective authors adopted their own assignments. We further add the investigation given by Schofield who discusses the long-lived MO^+ ion (M=metal atom) including LaO^+ where ions are expected to behave not like molecules but rather as atomic ions.[11] We will show in the present work that a single electron moves around the LaO^+ ion and the equilibrium molecular structure of LaO is determined substantially by LaO^+.

No previous investigations have been made using four-component relativistic theory. We therefore studied LaO using the four-component relativistic theory in order to establish the designations of the excited states.

Section II sets out the method of the calculations. Section III then discusses the electronic structures of LaO. Section IV offers concluding remarks.

II. METHOD OF CALCULATION

We used a reduced frozen-core approximation (RFCA) proposed by Matsuoka and Watanabe,[12,13] since this is a stable and timesaving method for treating molecules including the lanthanide atoms. The molecular basis sets used are La$[1^6+1^2/1^5+1^7/1^6+1^7/1^7+1^3/1^8/(1)]$+O$[21/421^3/(1)]$,

a)Electronic mail: htatewak@nsc.nagoya-cu.ac.jp.

TABLE I. Observed electronic states of LaO and their assignments.

St No.	Desig.			T_e (eV) Expt.[a]	T_0 (eV) Expt.[b]	Dominant configuration Berg[c]	Carette[b]	Kotzian[d]	Kaledin[e]	Shamps[f]
1	X	$^2\Sigma^+$	1/2	0.000	0.000		$6s^1$	$6s^1$	$6s^1$	$6s^1$
2	A′	$^2\Delta$	3/2	0.929	0.926			$5d^1$	$5d^1$	$5d^1$
3	A′	$^2\Delta$	5/2	1.016	1.013			$5d^1$	$5d^1$	$5d^1$
4	A	$^2\Pi$	1/2	1.570	1.567	$6p^1$		$6p^1$	$5d^1$	$5d^1$
5	A	$^2\Pi$	3/2	1.677	1.673	$6p^1$		$6p^1$	$5d^1$	$5d^1$
6	B	$^2\Sigma^+$	1/2	2.217	2.212	$6p^1$		$6p^1$	$5d^1$	$5d^1$
7	C	$^2\Pi$	1/2	2.806	2.804			$4f^1$	$6p^1$	
8	C	$^2\Pi$	3/2	2.833	2.832			$4f^1$	$6p^1$	
9	D	$^2\Sigma^+$	1/2	3.440	3.342		$7s^1$	$4f^1$	$6p^1$	
10	F	$^2\Sigma^+$	1/2	3.473	3.478		$8s^1$	$5d^1$		

[a]See Ref. 5.
[b]See Ref. 2.
[c]See Ref. 6.
[d]See Ref. 10.
[e]See Ref. 8.
[f]See Ref. 9.

where the slash symbol separates the symmetries s_+, p_-, p_+ (for La), $p_\pm$ (for O), $d_\pm$, $f_\pm$, and $g_\pm$ symmetries, 1^n indicates that n primitive Gaussian-type functions (pGTFs) are used, and the numbers 2 and 4 for the oxygen set indicate that the contracted GTFs (cGTF) are spanned with two and four primitives, respectively. The pGTFs to the left of + are those of the most diffuse GTFs determined by Koga *et al.*,[14,15] and the pGTFs to the right of + are the added diffuse pGTFs; for La, two s, seven p_-, seven p_+, and three d pGTFs are added in order to describe the Rydberg spinors. The symbol (1) for La denotes a single g-type polarization function and (1) for O is a single d-type polarization function.[16] The eight f-type primitives were generated previously.[17] Accordingly, the total number of molecular spinors generated is 183 for the large component. The numbers of the spinors and their Kramers' partners are in total 366.

We divide the electron shell groups into the following four categories:

(1) frozen-core, in which the spinors are fixed to the atomic ones;
(2) active core, from which single and double excitations are allowed, but are not treated as valence electrons in the complete active space configuration interaction (CASCI);
(3) valence shells, which are used to build CAS; and
(4) virtual shells, to which single and double excitations from the active core and the valence shells are permitted.

We first performed the Dirac–Hartree–Fock–Roothaan (DHFR) calculations. Our studies on the LaF (Ref. 18) and CeF molecules[19] showed that the spinor set obtained by solving DHFR for the system of one electron less than the target molecular system is appropriate for post-DHFR calculations. We therefore performed RFCA DHFR calculations for LaO^+. We next performed four-component relativistic CASCI (Ref. 20) for LaO, using the no-virtual-pair-approximation.[21–23] Then to take account of the correlation effects, four-component relativistic multiconfigurational quasidegenerate perturbation theory (MC-QDPT) calculations[24,25] were performed.

Previous studies of LaF^+ and LaF showed that it is vital to include correlation effects from the electrons in the $4s$, $4p$, $4d$, $5s$, and $5p$ spinors for analyzing the spectra. It is also necessary to include correlations from the $2s$ and $2p$ electrons of the F atom.[17] We therefore used frozen-core for LaO as the Zn^{2+}-like ion core of $La(1s^2\cdots3d^{10})$ and the He-like ion core of $O(1s^2)$.

To take account of the effect of the oxygen $2p$ electrons on molecular spectra, we prepared two types of active core, a large active core and a small active core.

The large active core is formally expressed as $[La^{3+}\ (4s^24p^64d^{10}5s^25p^6)\ O^{2-}(2s^22p^6)]^{1+}$ and actually as $[La^{1.6+}\ (4s^{2.0}4p^{6.0}4d^{10.0}5s^{2.0}5p^{5.8}p^{*0.2}d^{*1.2}f^{*0.3})\ O^{0.6-}\ (2s^{2.0}2p^{4.6})]^{1.0+}$ (see Sec. III). A single valence electron of LaO moves in the field generated by this active core. For the MC-QDPT calculation of LaO, the 183 spinors of LaO^+ are divided into the 17 active core, 25 valence, and 141 virtual spinors. The 25 valence spinors run from no. 18 to no. 42. The sums of s, p, d, and f GAOPs from no. 18 to no. 42 including the Kramers' partners are 5.6, 16.9, 27.5, and 0.9, respectively, indicating that these spinors can approximately describe $6s$-$8s$, $6p$-$8p$, and $5d$-$7d$-like spinors.

The small active core is formally expressed as $[La^{3+}\ (4s^24p^64d^{10}5s^25p^6)\ O^{4+}\ (2s^2)]^{7+}$, actually as $[La^{3.1+}\ (4s^{2.0}4p^{6.0}4d^{10.0}5s^{2.0}5p^{5.8}d^{*0.1})\ O^{3.9+}\ (2s^{1.9}2p^{0.2})]^{7.0+}$ and seven valence electrons are considered. For the MC-QDPT calculation of LaO, the 183 spinors of LaO^+ are divided into the 14 active core, 8 valence, and 161 virtual spinors. The numbers of the valence electrons and the valence spinors are restricted, since the resources for the post-DHFR calculations are limited.

We then performed CASCI and MC-QDPT calculations. The matrix element of MC-QDPT effective Hamiltonian is expressed by

TABLE II. Spinor energies (hartree), Ω, and GAOPs of LaO^+ at $R=3.45$ bohr.

No.	Spinor energy	Ω	La s_+	La p_-	La p_+	La d_-	La d_+	La f_-	La f_+	O s_+	O p_-	O p_+
1	−11.268 630	1/2	2.00	0.00	0.00	0.00	0.00	0.00	0.00	0.00	0.00	0.00
2	−9.022 515	1/2	0.00	2.00	0.00	0.00	0.00	0.00	0.00	0.00	0.00	0.00
3	−8.372 275	3/2	0.00	0.00	2.00	0.00	0.00	0.00	0.00	0.00	0.00	0.00
…	…	…	…	…	…	…	…	…	…	…	…	…
10	−1.984 305	1/2	1.92	0.00	0.00	0.00	0.00	0.00	0.00	0.06	0.01	0.02
11	−1.475 762	1/2	0.03	0.39	0.36	0.01	0.01	0.00	0.00	1.13	0.02	0.05
12	−1.260 614	1/2	0.00	1.43	0.46	0.00	0.00	0.00	0.00	0.09	0.01	0.01
13	−1.190 419	3/2	0.00	0.00	1.98	0.00	0.00	0.00	0.00	0.00	0.00	0.02
14	−1.085 699	1/2	0.03	0.13	1.04	0.02	0.04	0.00	0.00	0.65	0.05	0.05
	$\Sigma GAOP_{i\lambda}$(i=1 to 14)		3.98	3.94	7.82	4.03	6.05	0.01	0.01	1.92	0.08	0.15
					La:25.842 (La $5p^{5.76}$)						O:2.158 ($2p^{0.23}$)	
15	−0.618 661	1/2	0.00	0.01	0.01	0.20	0.11	0.05	0.03	0.00	0.97	0.60
16	−0.616 468	3/2	0.00	0.00	0.02	0.07	0.25	0.02	0.06	0.00	0.00	1.57
17	−0.592 235	1/2	0.02	0.05	0.12	0.16	0.28	0.03	0.04	0.03	0.49	0.77
	$\Sigma GAOP_{i\lambda}$(i=15 to 17)		0.02	0.06	0.15	0.44	0.65	0.10	0.14	0.03	1.46	2.94
					La:1.562 (La $p^{*0.21}d^{*1.08}f^{*0.24}$)						O:4.438 ($2p^{4.40}$)	
	$\Sigma GAOP_{i\lambda}$(i=1 to 17)		4.00	4.00	7.98	4.47	6.70	0.11	0.14	1.95	1.55	3.09
	Total GAOP				La:27.404 (La $p^{*0.21}d^{*1.17}f^{*0.26}$)						O:6.596 ($2p^{4.63}$)	
18	−0.174 165	1/2	1.68	0.10	0.17	0.02	0.03	0.00	0.00	0.00	0.00	0.00
19	−0.124 708	3/2	0.00	0.00	0.00	1.61	0.37	0.02	0.01	0.00	0.00	0.00
20	−0.123 142	5/2	0.00	0.00	0.00	0.00	1.98	0.00	0.02	0.00	0.00	0.00
21	−0.121 421	1/2	0.00	0.99	0.41	0.37	0.16	0.01	0.00	0.00	0.04	0.03
22	−0.118 553	3/2	0.00	0.00	1.39	0.08	0.44	0.00	0.01	0.00	0.00	0.07
23	−0.096 957	1/2	0.11	0.23	0.67	0.32	0.60	0.01	0.02	0.00	0.02	0.03
24	−0.066 892	1/2	1.65	0.10	0.14	0.04	0.06	0.00	0.00	0.00	0.01	0.01
25	−0.063 374	1/2	0.00	0.70	0.33	0.58	0.39	0.11	0.09	0.00	−0.14	−0.06
26	−0.063 074	3/2	0.00	0.00	1.00	0.19	0.81	0.06	0.14	0.00	0.00	−0.20
27	−0.051 847	1/2	0.01	0.72	0.19	0.82	0.42	0.01	0.01	0.00	−0.12	−0.07
28	−0.051 233	3/2	0.00	0.00	0.93	0.25	0.98	0.00	0.01	0.00	0.00	−0.17
29	−0.049 154	1/2	0.19	0.32	1.05	0.13	0.29	0.02	0.02	0.00	−0.02	0.00
…	…	…	…	…	…	…	…	…	…	…	…	…
41	−0.024 713	1/2	0.07	0.09	0.18	0.65	1.08	0.01	0.02	0.00	−0.04	−0.06
42	−0.023 143	1/2	0.00	0.78	0.42	0.47	0.30	0.02	0.01	0.00	0.00	0.00
	$\Sigma GAOP_{i\lambda}$(i=18 to 42)		5.64	6.05	10.86	11.19	16.30	0.36	0.50	0.00	−0.34	−0.55

$$H_{\mu\nu} = E_{\mu}^{\mathrm{CASCI}}\delta_{\mu\nu} + \frac{1}{2}\left\{\sum_{I\notin \mathrm{CAS}} \frac{\langle\mu|H_{\mathrm{DC}}^{+}|I\rangle\langle I|H_{\mathrm{DC}}^{+}|\nu\rangle}{E_{\nu}^{(0)} - E_{I}^{(0)}} + (\mu \leftrightarrow \nu)^{*}\right\}, \quad (1)$$

where μ and ν denote CASCI eigenfunctions, and $E_i^{(0)}$ is the zeroth order energy of the state i. Single and double excitations from the active core and valence shells to all the valence and virtual shells are taken into account. In the DHFR calculation the $C_{\infty v}$ double group is used, but in the CASCI and MC-QDPT calculations the symmetry restriction is not imposed, although the molecular integrals are evaluated in the $C_{\infty v}$ double group.

Using the potential energy curves given by MC-QDPT, we obtained the spectroscopic constants of the equilibrium nuclear distance (R_e) and the vibrational frequency (ω_e) and the energy difference (T_0) between the lowest vibrational level of the ground state and that of the excited state.

All the programs discussed above (RFCA-DHFR,[12,13] CASCI, and MC-QDPT[24,25]) were developed by the theoretical group of Kyushu University including two of the present authors (Y.W. and H.N.).

III. RESULTS

A. DHFR calculation

As explained, we performed RFCA DHFR calculations for LaO^+. The DHFR total energy for LaO^+ is −8568.5182 hartree at the experimental equilibrium nuclear distance of the LaO ground state ($R_e=3.45$ bohr). The spinor energies, total electronic angular momentum around the molecular axis (Ω), and the gross atomic orbital populations (GAOPs) (Ref. 26) for LaO^+ at R_e are set out in Table II, and the contour maps for the important spinors (nos. 15–21 spinors in Table II) are shown in Fig. 1.

We recall that the formal electron numbers for La and O are, respectively, 26 and 8 in RFCA calculations. Table II shows that the total electrons in a large active core are 27.4 and 6.6 for La and O, respectively; in LaO^+, 1.4 electrons in O $2p$ move into La p^*, d^*, and f^* spinors

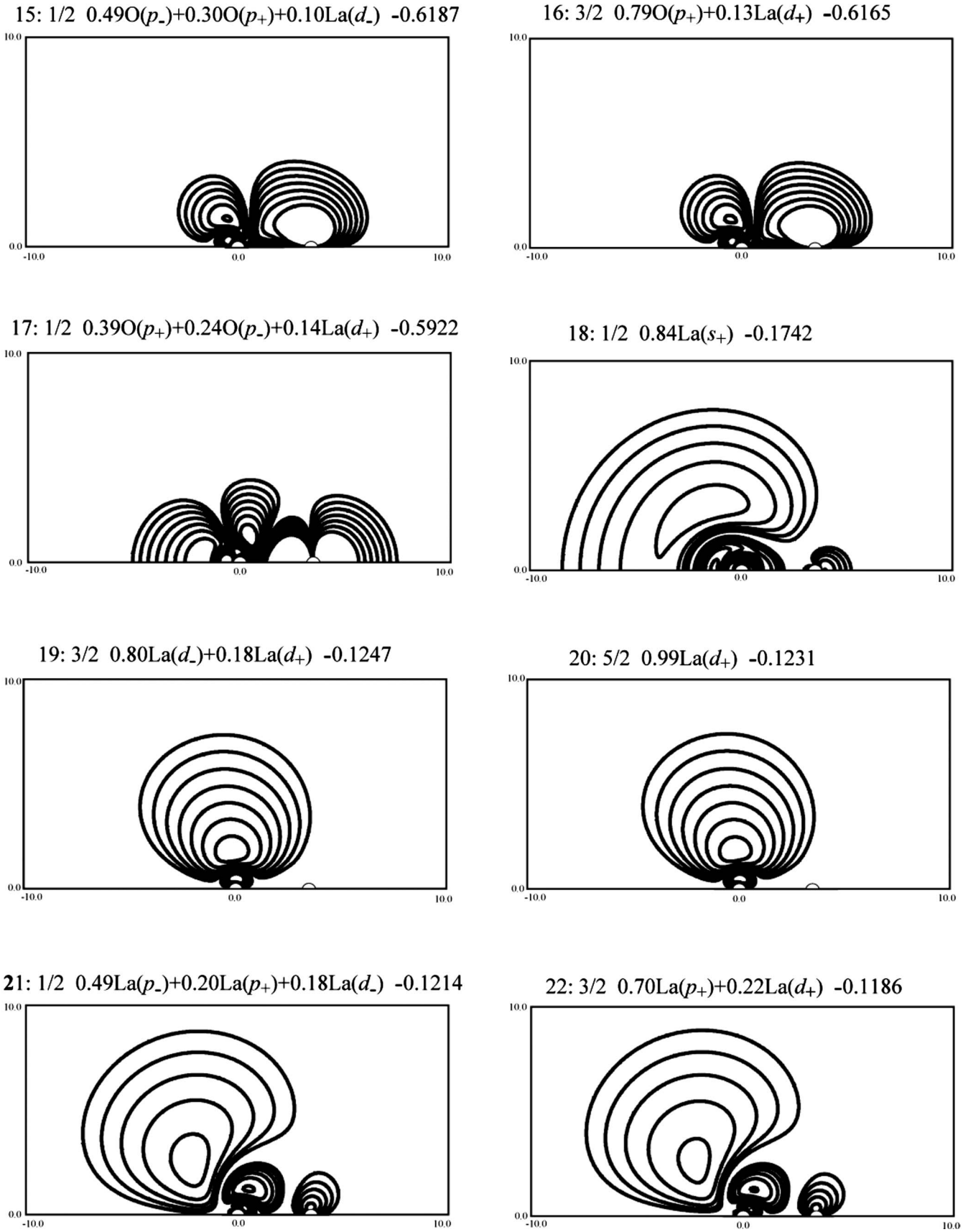

FIG. 1. Contour maps of densities of the important valence spinors of the ground state LaO^+. The spinor numbers (no.), Ω, the characters with GAOPs (···), and the spinor energies in hartree (ε) are given in the respective contour maps as no: Ω, (···), ε The horizontal and vertical (*z*- and *x*-) axes are in bohr; *z* covers −10 to 10 bohr and *x* 0–+10 bohr. The circles on the *z*-axis at *z*=0.0 and 3.45 bohr indicate the La and O nuclei, respectively. The outermost values of the contour line are 0.0001 *e* $bohr^{-3}$. The value of an inner line is twice as large as that of its neighboring outer line. The electron numbers inside the outermost line are between 0.963 and 1.000.

TABLE III. Vertical excitation energies, Ω, dominant CSF and GAOP at R=3.45 bohr from MC-QDPT with large and small active core for LaO.

Expt.				Large active core (1 valence electron)				Small active core (7 valence electrons)			
Desig.		T_0	Ω	ΔE (eV)	Ω	Dominant CSF[a]	GAOP[b]	ΔE (eV)	Ω	Dominant CSF	GAOP[c]
								−62.472[d]	1/2	◆Excitation from O to La	$s^{0.8}p^{0.1}d^{0.8}f^{0.0}(p^*d^*f^*\mathrm{O}\ 2p)^{5.4}$
X	$^2\Sigma^+$	0.000	1/2	0.000[e]	1/2	$0.99\|18\|+\cdots$	$s^{0.8}p^{0.1}d^{0.0}f^{0.0}2p^{0.0}$	0.000[f]	1/2	$1.00\|18\|+\cdots$	$s^{0.8}p^{0.1}d^{0.0}f^{0.0}(p^*d^*f^*\mathrm{O}\ 2p)^{6.0}$
A′	$^2\Delta$	0.926	3/2	0.989	3/2	$0.97\|19\|+0.19\|\underline{19}\|+\cdots$	$s^{0.0}p^{0.0}d^{1.0}f^{0.0}2p^{0.0}$	0.988	3/2	$1.00\|19\|+\cdots$	$s^{0.0}p^{0.0}d^{1.0}f^{0.0}(p^*d^*f^*\mathrm{O}\ 2p)^{6.0}$
A′	$^2\Delta$	1.013	5/2	1.091	5/2	$0.98\|20\|+0.17\|\underline{20}\|+\cdots$	$s^{0.0}p^{0.0}d^{1.0}f^{0.0}2p^{0.0}$	1.077	5/2	$0.88\|20\|-0.45\|\underline{20}\|+\cdots$	$s^{0.0}p^{0.0}d^{1.0}f^{0.0}(p^*d^*f^*\mathrm{O}\ 2p)^{6.0}$
								1.085	1/2	◆Excitation from O to La	$s^{1.5}p^{0.3}d^{-0.1}f^{0.0}(p^*d^*f^*\mathrm{O}\ 2p)^{5.4}$
A	$^2\Pi$	1.567	1/2	1.718	1/2	$0.98\|21\|+\cdots$	$s^{0.0}p^{0.7}d^{0.3}f^{0.0}2p^{0.0}$	1.699	1/2	$0.87\|21\|-0.49\|\underline{21}\|+\cdots$	$s^{0.0}p^{0.7}d^{0.3}f^{0.0}(p^*d^*f^*\mathrm{O}\ 2p)^{6.0}$
A	$^2\Pi$	1.673	3/2	1.843	3/2	$0.81\|22\|+0.56\|\underline{22}\|+\cdots$	$s^{0.0}p^{0.7}d^{0.3}f^{0.0}2p^{0.0}$	1.806	3/2	$0.93\|22\|+0.37\|\underline{22}\|+\cdots$	$s^{0.0}p^{0.7}d^{0.3}f^{0.0}(p^*d^*f^*\mathrm{O}\ 2p)^{6.0}$
								1.949	5/2	◆Excitation from O to La	$s^{0.7}p^{0.2}d^{0.7}f^{0.0}(p^*d^*f^*\mathrm{O}\ 2p)^{5.4}$
								2.567	5/2	◆Excitation from O to La	$s^{0.8}p^{0.1}d^{0.8}f^{0.0}(p^*d^*f^*\mathrm{O}\ 2p)^{5.4}$
B	$^2\Sigma^+$	2.212	1/2	2.520	1/2	$0.98\|23\|+\cdots$	$s^{0.1}p^{0.5}d^{0.4}f^{0.0}2p^{0.0}$	2.622	7/2	◆Excitation from O to La	$s^{0.8}p^{0.1}d^{0.8}f^{0.0}(p^*d^*f^*\mathrm{O}\ 2p)^{5.4}$
C	$^2\Pi$	2.804	1/2	3.362	1/2	$0.84\|25\|+0.43\|\underline{25}\|+\cdots$	$s^{0.0}p^{0.5}d^{0.5}f^{0.1}2p^{-0.1}$	3.206	5/2	◆Excitation from O to La	$s^{0.8}p^{0.1}d^{0.8}f^{0.0}(p^*d^*f^*\mathrm{O}\ 2p)^{5.4}$
C	$^2\Pi$	2.832	3/2	3.404	3/2	$0.72\|26\|+0.63\|\underline{26}\|+\cdots$	$s^{0.0}p^{0.5}d^{0.5}f^{0.1}2p^{-0.1}$	4.136	1/2	◆Excitation from O to La	$s^{0.8}p^{0.7}d^{0.1}f^{0.0}(p^*d^*f^*\mathrm{O}\ 2p)^{5.4}$
D	$^2\Sigma^+$	3.157	1/2	3.635	1/2	$0.99\|24\|+\cdots$	$s^{0.8}p^{0.1}d^{0.1}f^{0.0}2p^{0.0}$	4.804	3/2	◆Excitation from O to La	$s^{0.8}p^{0.1}d^{0.8}f^{0.0}(p^*d^*f^*\mathrm{O}\ 2p)^{5.4}$
F	$^2\Sigma^+$	3.554	1/2	4.068	1/2	$0.74\|29\|+0.62\|27\|+\cdots$	$s^{0.1}p^{0.6}d^{0.4}f^{0.0}2p^{0.0}$	4.983	1/2	◆Excitation from O to La	$s^{0.8}p^{0.7}d^{0.1}f^{0.0}(p^*d^*f^*\mathrm{O}\ 2p)^{5.4}$
			1/2	4.101	1/2	$0.77\|27\|-0.61\|29\|+\cdots$	$s^{0.0}p^{0.5}d^{0.5}f^{0.0}2p^{-0.1}$	5.188	3/2	◆Excitation from O to La	$s^{0.8}p^{0.1}d^{0.8}f^{0.0}(p^*d^*f^*\mathrm{O}\ 2p)^{5.4}$

[a]|N| and |N̲| mix each other in the present CASCI and MC-QDPT calculations where 25 valence spinors (spin partners+Kramers' partners=50) are employed, since |N| and |N̲| are degenerated (we confirmed that CASCI calculations with Ω=X gives the same TEs as those with Ω=X plus X̲.). MC-QDPT gives slightly different TEs calculated with Ω=X or Ω=X plus X̲, since the number of the virtual spinors and the resulting correlating spaces differ in the two calculations. We, however, found that MC-QDPT calculations with Ω=X and Ω=X plus X̲ give almost the same excitation energies.
[b]The symbol $2p$ indicates O $2p$.
[c]The symbol $(p^*d^*f^*\mathrm{O}\ 2p)^{x.x}$ indicates the sum of GAOPS of the three highest spinors 15, 16, and 17 composed of the La p^*,d^*,f^* spinors, and O $2p$. In the case of $(p^*d^*f^*\mathrm{O}\ 2p)^{6.0}$, O $2p$ GAOPs are 4.4, while of $(p^*d^*f^*\mathrm{O}\ 2p)^{5.4}$, O $2p$ GAOPS are 3.8.
[d]The total energy of the first state of the small active-core calculation is −8572.281 426 hartree.
[e]The total energy of the first state of the large active-core calculation is −8570.006 457 hartree.
[f]The total energy of the second state of the small active-core calculation is −8569.985 632 hartree.

forming $[\mathrm{La}^{1.6+}\ (4s^{2.0}4p^{6.0}4d^{10.0}5s^{2.0}5p^{5.8}p^{*0.2}d^{*1.2}f^{*0.3})\ \mathrm{O}^{0.6-}\ (2s^{2.0}2p^{4.6})]^+$, where p^*, d^*, and f^* are the polarization functions of La that form three molecular spinors with O $2ps$: we use p^*, d^*, and f^* instead of $6p$, $5d$, and $4f$, since as indicated from nos. 15–17 they are different from the atomiclike spinors (see the charge densities around the La nucleus). We see from Fig. 1 and Table II that the O $2p$ electrons penetrate into the La core region using the p^*, d^*, and f^* spinors. The next paragraph shows the validity to use LaO^+ DHFR spinors for investigating the LaO spectra.

The dissociation energy (D_e) calculated for LaO^+ with MC-QDPT is close to that for LaO. The D_e value for LaO^+, where 6 electrons in O $2p$ are considered, is 6.58 eV at calculated R_e of 3.37 bohr, and D_e for LaO where 7 electrons (O $2p$ 6 electrons+La $6s$ electron) are considered is 6.85 eV at calculated R_e of 3.49 bohr. This implies that the added single electron participates only slightly in the formation of chemical bond of LaO; the one electron moves in the field generated from $[\mathrm{La}^{1.6+}\ (4s^{2.0}4p^{6.0}4d^{10.0}5s^{2.0}5p^{5.8}p^{*0.2}d^{*1.2}f^{*0.3})\ \mathrm{O}^{0.6-}\ (2s^{2.0}2p^{4.6})]^+$.

We thus see that it is adequate to use LaO^+ DHFR spinors for calculating LaO electronic state. We, however, add that on the contrary to the calculation, the experimental D_es are 8.89 eV (Ref. 11) and 8.23 eV (Ref. 5) for LaO^+ and LaO, respectively, indicating that the added electron slightly weakens the chemical bond. Further investigation is necessary to clarify the role of the $6s$-like electron, but this is beyond the scope of the present work.

As indicated from GAOPs in Table II, the chemical bond is mainly formed with La p^*, d^*, and f^* and O $2p$, and is partially formed with La $5p$ and O $2s$ as the GdF molecule.[27] Wahlgren *et al.*[28] also discussed that U $6s$ and $6p$ electrons in $\mathrm{UO_2}^{2+}$ are highly polarizable and interact with O $2s$ and $2p$ electrons. A similar bonding as LaO is found also in ThO where the bonding primarily takes places between the $6d$ and the O $2p_\sigma$ orbitals whereas the $7s$-electrons construct a diffuse lone pair.[29]

The LFT calculations[2,8,9] all assume that LaO^+ takes the electronic configuration $[\mathrm{La}^{3+}\ (4s^2\cdots5p^6)\ \mathrm{O}^{2-}\ (2s^22p^6)]^+$. The validity of this assumption will be discussed later.

B. CASCI and MC-QDPT calculations for LaO

1. Large active-core calculations

Table III shows the vertical excitation energies (ΔE), Ω, dominant CSF and approximate GAOPs given by the large active core and small active-core calculations at the experimental value of R_e (3.45 bohr). In the column of the dominant CSF, the number in the Slater determinant |N| denotes the singly occupied spinors in Table II. The doubly occupied nos. 1–17 spinors are not shown. For example, |18| denotes the Slater determinant arising from the $1^2\cdots15^216^217^218^1$ electronic configuration. A number underlined such as N̲ indicates the Kramers' partner of the spinor "N."

TABLE IV. The excitation energies and GAOPs of CASCI at $R=3.45$ bohr.

St.	RFCA-CASCI			All-electron-CASCI (DIRAC)				
No.	ΔE (eV)	Ω	GAOP	ΔE (eV)	Ω	TRDM (D)[a]	TRPB[b]	GAOP
1	0.000[c]	1/2	$s^{0.8}p^{0.1}d^{0.0}f^{0.0}(p^*d^*f^*\mathrm{O}\ 2p)^{6.0}$	0.000[d]	1/2			$s^{0.8}p^{0.1}d^{0.0}f^{0.0}(p^*d^*f^*\mathrm{O}\ 2p)^{6.1}$
2	1.346	3/2	$s^{0.0}p^{0.0}d^{1.0}f^{0.0}(p^*d^*f^*\mathrm{O}\ 2p)^{6.0}$	1.347	3/2	0.25[e]	0.02	$s^{0.0}p^{0.0}d^{0.9}f^{0.0}(p^*d^*f^*\mathrm{O}\ 2p)^{6.1}$
3	1.390	5/2	$s^{0.0}p^{0.0}d^{1.0}f^{0.0}(p^*d^*f^*\mathrm{O}\ 2p)^{6.0}$	1.390	5/2	F[f]		$s^{0.0}p^{0.0}d^{0.9}f^{0.0}(p^*d^*f^*\mathrm{O}\ 2p)^{6.1}$
4	1.439	1/2	$s^{0.0}p^{0.7}d^{0.3}f^{0.0}(p^*d^*f^*\mathrm{O}\ 2p)^{6.0}$	1.439	1/2	7.80	29.87	$s^{0.0}p^{0.7}d^{0.2}f^{0.0}(p^*d^*f^*\mathrm{O}\ 2p)^{6.1}$
5	1.518	3/2	$s^{0.0}p^{0.7}d^{0.3}f^{0.0}(p^*d^*f^*\mathrm{O}\ 2p)^{6.0}$	1.518	3/2	7.43	31.74	$s^{0.0}p^{0.7}d^{0.2}f^{0.0}(p^*d^*f^*\mathrm{O}\ 2p)^{6.1}$
6	6.258	1/2	$s^{1.5}p^{0.3}d^{-0.1}f^{0.0}(p^*d^*f^*\mathrm{O}\ 2p)^{5.4}$	6.249	1/2	0.61	15.11	$s^{1.5}p^{0.3}d^{-0.1}f^{-0.1}(p^*d^*f^*\mathrm{O}\ 2p)^{5.5}$
7	6.506	1/2	$s^{0.8}p^{0.1}d^{0.8}f^{0.0}(p^*d^*f^*\mathrm{O}\ 2p)^{5.4}$	6.505	1/2	0.11	0.53	$s^{0.8}p^{0.0}d^{0.7}f^{-0.1}(p^*d^*f^*\mathrm{O}\ 2p)^{5.5}$
8	6.528	3/2	$s^{0.8}p^{0.1}d^{0.8}f^{0.0}(p^*d^*f^*\mathrm{O}\ 2p)^{5.4}$	6.526	3/2	0.06	0.18	$s^{0.8}p^{0.0}d^{0.7}f^{-0.1}(p^*d^*f^*\mathrm{O}\ 2p)^{5.5}$
9	6.553	5/2	$s^{0.8}p^{0.1}d^{0.8}f^{0.0}(p^*d^*f^*\mathrm{O}\ 2p)^{5.4}$	6.551	5/2	F		$s^{0.8}p^{0.0}d^{0.7}f^{-0.1}(p^*d^*f^*\mathrm{O}\ 2p)^{5.5}$
10	6.582	7/2	$s^{0.8}p^{0.1}d^{0.8}f^{0.0}(p^*d^*f^*\mathrm{O}\ 2p)^{5.4}$	6.580	7/2	F		$s^{0.8}p^{0.0}d^{0.7}f^{-0.1}(p^*d^*f^*\mathrm{O}\ 2p)^{5.5}$
11	6.763	3/2	$s^{0.8}p^{0.1}d^{0.8}f^{0.0}(p^*d^*f^*\mathrm{O}\ 2p)^{5.4}$	6.760	3/2	0.04	0.07	$s^{0.8}p^{0.0}d^{0.7}f^{-0.1}(p^*d^*f^*\mathrm{O}\ 2p)^{5.5}$
12	6.817	5/2	$s^{0.8}p^{0.1}d^{0.8}f^{0.0}(p^*d^*f^*\mathrm{O}\ 2p)^{5.4}$	6.813	5/2	F		$s^{0.8}p^{0.0}d^{0.7}f^{-0.1}(p^*d^*f^*\mathrm{O}\ 2p)^{5.5}$

[a]The symbol F indicates that the transition between the ground state ($\Omega=1/2$) to this state is forbidden.
[b]TRPB is transition probability in 10^6 s^{-1}.
[c]Total energy for the ground state is −8568.693 162 hartree.
[d]Total energy for the ground state is −8568.702 165 hartree.
[e]Although TRDM from the ground state to the second state is small (0.25 D), TRDM between second and fourth state is 5.60 D.
[f]Although the transition between the ground state ($\Omega=1/2$) to the third state ($\Omega=5/2$) is forbidden, TRDM between third and fifth state is 5.68 D.

The GAOPs in Table III are approximate ones given in the form $(\lambda)^{\mathrm{GAOP}_\lambda}(\lambda=s,\ p,\ d,\ \text{and}\ f)$

$$\mathrm{GAOP}_\lambda = \Sigma C_i^2 \mathrm{GAOP}_{i\lambda}, \tag{2}$$

where λ, i, and C_i, respectively, denote the symmetry of the atomic spinor, the configuration, and the mixing configurational coefficient in MC-QDPT.

We first discuss the results of the large active-core (1 valence electron) calculations. The first state of the large active-core calculation is $6s^1$-like (dominant CSF is $0.99|18|$), which is consistent with the experimental ground state. The calculated energy difference between the first and the second state is 0.989 eV. This is very close to the experimental excitation energy T_0 of the $A'\ ^2\Delta_{3/2}$ (0.926 eV). Moreover, in the large active-core calculation, the calculated vertical excitation energies of other states are also close to the experimental T_0s of the $A'(^2\Delta_{5/2})$, A and B states. The assignments given by the large active-core calculation are very different from those of other authors; the ground, two A′, and D states are pure s or d-like states, and all others are p-d hybridized ones, as shown in the seventh column of Table III.

2. Small active-core calculations and intruder-induced states

We now discuss the results of the small active-core (7 valence electrons) calculation. As seen in Table III, the total energy of the first state of the small active-core calculation is extremely low (−8572.2814 hartree). We therefore suspect that this state does not exist. The total energy of the second state (−8569.9856 hartree) is very close to that of the first state of the large active-core calculation (−8570.0065 hartree). The first state of the small active-core calculation originates from a single excitation from O $2p$ to La $5d$. The second state of the small active-core calculation has the same GAOP as the first state of the large active-core calculation. We suspect that the first state of the small active-core calculation is induced by intruder states.[30,31] We mark with a diamond (♦) those states which are suspected to be intruder-induced states.

To avoid contamination of the intruder states, we introduced an energy denominator shift parameter δ; we replaced $E_\nu^{(0)}-E_I^{(0)}$ in Eq. (1) with $E_\nu^{(0)}-E_I^{(0)}+\delta/(E_\nu^{(0)}-E_I^{(0)})$.[31] We performed the small active-core calculation at the experimental value of R_e, changing δ from 0.0 to 0.2 and found that all the states with ♦ in Table III are intruder-induced states.

Schamps *et al.*[9] found some states with an O $2p$ hole between 1.2 and 2.1 eV in their MRCI calculations that were missing in the LFT. In subsection B-3, we shall show that these states lie about 5 eV above the ground state.

3. Non-existence of states with an O 2p hole below 5 eV

To study the states with an O $2p$ hole in more detail, we performed all-electron CASCI with the DIRAC program,[32] and calculated the magnitudes of the transition dipole moment (TRDM).[33] The basis set used to calculate the TRDM is the same as the present one, except for adding the pGTFS for the La $1s$-$3d$ and O $1s$ spinors which are treated as the frozen core in the previous RFCA calculations. The seven electrons are distributed in the spinors corresponding to nos. 15 to 22 in Table I. The results are shown in Table IV. The total energies of the ground states are −8568.693 162 and −8568.702 165 hartree for RFCA CASCI and all-electron CASCI calculations. These are very close to each other. The

calculated excitation energies ΔE and the GAOPs show complete agreement, and we found that the charge-transferred excited states from O to La lie energetically far from the ground state in the CASCI. Table IV also shows that TRDMs from the ground state to the second, fourth, and fifth state which have $(p^*d^*f^*\text{O } 2p)^{6.0-6.1}$ are, respectively, 0.3, 7.8, and 7.4 D. In contrast, TRDMs from the ground state to the seventh and upper states with $(p^*d^*f^*\text{O } 2p)^{5.4-5.5}$ are much smaller than TRDMs from the ground state to the states with $(p^*d^*f^*\text{O } 2p)^{6.0-6.1}$. We recognize, however, that the TRDM and the transition probability (TRPB) from the sixth state are large. This indicates that the state with $[\text{La } 6s^{1.5}6p^{0.3}5d^{-0.1}4f^{0.0}(p^*d^*f^*\text{O } 2p)^{5.4}]$ configuration may be observed in the very high energy region, above 5 eV.

Using the DIRAC program, we performed restricted active space configuration interaction (RASCI) calculations in which single and double excitations are permitted from the CAS space (nos. 15–22) to the virtual space (nos. 23–35). We found that the lower states are almost equivalent to those of the MC-QDPT calculation using the large active-core. The states with an O $2p$ hole by RASCI are at least 5.2 eV above the ground state (see Appendix).

We conclude that we can disregard the states with O $2p \rightarrow$ La when analyzing the experimental spectra below 5 eV.

C. Assignments and spectroscopic constants

1. Potential energy curves, excitation energies, and assignments

We performed the small and large active-core calculations at eight points from 2.75 to 4.5 bohr, and drew the corresponding potential energy curves. We took $\delta = 0.000\,08$ to avoid the intruder states in MC-QDPT; this value of δ was used in previous LnF calculations (see Refs. 17–19). As mentioned above, we threw away the states with $(p^*d^*f^*\text{O } 2p)^{5.4}$ in the small active-core calculations.

Table V shows the excitation energies (T_0) and the approximate configurations and the spectroscopic constants (to be discussed in subsection C-2) of MC-QDPT calculations. The assignments by Kotzian *et al.*[10] and Kaledin *et al.*[8] are also included in Table V.

The ground state is $^2\Sigma^+_{1/2}$. Its configuration is $[\text{La}(5p^{5.76}6s^{0.83}6p^{0.14}p^{*0.21}d^{*1.17}f^{*0.26})\ \text{O}(2p^{4.63})]$ abbreviated as $[6s^{0.83}6p^{0.14}(p^*d^*f^*\text{O } 2p)^{6.03}]$. Experimentally, two states are observed, at 0.93 eV and 1.01 eV above the ground state, and these are designated as $A'\ ^2\Delta$ with $\Omega = 3/2$ and 5/2. In the small active-core calculation, the T_0s of the second and third states are 0.93 and 1.03 eV, respectively. Thus we have successfully reproduced the experimental $A'\ ^2\Delta$ excitation energies. In the large active-core calculation, the T_0s of the second and third states are 0.89 and 1.00 eV. Both calculations show that the configurations of the second and third states are $(d)^1_{3/2}$ and $(d)^1_{5/2}$. We also confirm these assignments by inspecting the shapes of the pure d-like nos. 19 and 20 spinors included in the A′ states (see Tables II and III and Fig. 1).

The fourth and fifth states are experimentally designated as $A\ ^2\Pi$ with $\Omega = 1/2$ and 3/2. The calculated T_0s of the

TABLE V. Excitation energies and assignment of states and spectroscopic constants from MC-QDPT for LaO.

St	Expt.			T_0 (eV)		R_e (bohr)			ω_e (cm^{-1})			D_e (eV)		Approximated configuration		
No.	Desig.	Ω	Expt.	Small actv-core (7 val. el.)	Large actv-core (1 val. el.)	Expt.	Small actv-core (7 val. el.)	Large aactv-core (1 val. el.)	Expt.	Small actv-core (7 val. el.)	Large actv-core (1 val. el.)	Expt.	Small actv-core (7 val. el.)	Large actv-core (1 val. el.)	This work	Kotzian[a]	Kaledin[b]
1	X $^2\Sigma^+$	1/2	0.000	0.000	0.000	3.449	3.493	3.578	817.3	822.6	706.6	8.23	6.80[c]	7.44[c]	$6s^1$	$6s^1$	$6s^1$
2	A′ $^2\Delta$	3/2	0.926	0.926	0.888	3.492	3.568	3.669	768.2	714.7	612.8		5.92[d]	6.60[d]	$5d^1$	$5d^1$	$5d^1$
3	A′ $^2\Delta$	5/2	1.013	1.031	0.998	3.492	3.567	3.663	773.9	703.0	617.3		5.79[e]	6.47[e]	$5d^1$	$5d^1$	$5d^1$
4	A $^2\Pi$	1/2	1.567	1.664	1.688	3.477	3.542	3.610	756.5	675.2	655.9		5.13[c]	5.75[c]	(hybridized-pd)^1	$6p^1$	$5d^1$
5	A $^2\Pi$	3/2	1.673	1.782	1.818	3.477	3.540	3.605	754.2	671.1	657.3		5.06[d]	5.67[d]	(hybridized-pd)^1	$6p^1$	$5d^1$
6	B $^2\Sigma^+$	1/2	2.212		2.452	3.505		3.646	732.9		623.3			4.99[c]	(hybridized-pd)^1	$6p^1$	$5d^1$
7	C $^2\Pi$	1/2	2.804		3.371	3.456		3.570	792.4		702.8			4.07[c]	(hybridized-pd)^1	$4f^1$	$6p^1$
8	C $^2\Pi$	3/2	2.832		3.412	3.456		3.569	801.1		709.4			4.07[d]	(hybridized-pd)^1	$4f^1$	$6p^1$
9	D $^2\Sigma^+$	1/2	3.157		3.706			3.466			810.0			3.73[c]	$7s^1$	$4f^1$	$6p^1$
10	F $^2\Sigma^+$	1/2	3.554		4.135			3.475			779.7			3.31[c]	(hybridized-pd)^1	$5d^1$	
11		1/2			4.176			3.460			864.6			3.26[c]	(hybridized-pd)^1		

[a]See Ref. 10.
[b]See Ref. 8.
[c]In obtaining D_e's we assume that LaO ($\Omega = 1/2$) dissociates into La ($\Omega = 3/2$) with −8494.7327 and O ($\Omega = 2$) with −75.0010 hartree.
[d]In obtaining D_e's we assume that LaO ($\Omega = 3/2$) dissociates into La ($\Omega = 3/2$) with −8494.7327 and O ($\Omega = 0$) with −74.9994 hartree.
[e]In obtaining D_e's we assume that LaO ($\Omega = 5/2$) dissociates into La ($\Omega = 3/2$) with −8494.7327 and O ($\Omega = 1$) with −75.0001 hartree.

A $^2\Pi_{1/2}$ are 1.66 and 1.69 eV for the small and large active-core calculations, respectively, and it is 1.57 eV experimentally. The calculated T_0s of the A $^2\Pi_{3/2}$ are 1.78 and 1.82 eV for the small and large active-core calculations, respectively, and 1.67 eV experimentally. Although Kotzian *et al.*[10] assigned the A states as $(6p)^1$, and Kaledin *et al.*[8] as $(5d)^1$, this work shows that the $^2\Pi_{1/2}$ is assigned as $(\text{hybridized-}6p5d)^1_{1/2}$ and $^2\Pi_{3/2}$ is assigned as $(\text{hybridized-}6p5d)^1_{3/2}$.

The large active-core calculation indicates that the sixth state corresponding to the experimentally assigned B $^2\Sigma^+$ has T_0 2.45 eV and a $(\text{hybridized-}6p5d)^1_{1/2}$ configuration resulting from the no. 23 spinor. In the small active-core calculation, we cannot include spinors equal to or higher than no. 23, and consequently the excited states equal to or higher than B states are not generated.

The lowest $4f$ spinor, which has a positive spinor energy (not shown in Table II, because of the high spinor energy), is no. 60 of the LaO^+ DHFR spinors. We see no excited states with $4f$ spinors below 6 eV. Although Kotzian *et al.* designated the C and D states as $^2\Pi_{1/2}(4f)^1$, $^2\Pi_{3/2}(4f)^1$, and $^2\Sigma_{1/2}(4f)^1$,[10] we propose C as $(\text{hybridized-}6p5d)^1_{1/2}$ and $(\text{hybridized-}6p5d)^1_{3/2}$, and D as $(7s)^1_{1/2}$. The assignment of the F state by Carette[2] as $(8s)^1$ is also questionable (see Table I). We propose F as $(\text{hybridized-}6p5d)^1_{1/2}$, since the $8s$ spinor, which is no. 35 spinor of the LaO^+ DHFR calculation (not shown in Table II), has a higher spinor energy (-0.03 hartree) than those of spinors 27 and 29 composing the F state (see Tables I and III).

2. Spectroscopic constants

The spectroscopic constants are collected in Table V. The dissociation energies (D_e) are 8.23 eV experimentally,[5] and 6.80 and 7.44 eV according to the small and large active-core calculations, respectively. The agreement in D_e between experiment and the value calculated with the small active-core is moderate.

The experimental and calculated R_e values agree well. For example, R_e for the ground state is 3.45 bohr experimentally, and 3.49 and 3.58 bohr for the small and large active-core calculations, respectively. The small active-core (7 valence electrons) calculation gives much better ω_e values than the large active-core (1 valence electron) calculation as for R_e. The ω_e values for the ground state, for example, are 817 cm^{-1} experimentally, and 822 and 707 cm^{-1} for the small and large active core calculations, respectively. However, as mentioned above, the small active-core calculation cannot treat states equal to or higher than B, since the limitation of computer resources restricts the number of valence spinors to 9.

Finally, we discuss the foundation of the LFT calculations.[2,8,9] Since the excitations from O $2p$ spinors can be neglected in analyzing the experimental spectra of the lower excited states, we may choose the large active-core calculation instead of the small active-core calculation. Equivalently, we see that in LaO a single valence electron moves around the $La^{1.6+}$ $O^{0.6-}$ ion core and the electron is localized at the La atom for the lower excited states. We can therefore discuss the electronic structure of the molecule by considering only one valence electron, if we can take account of the correlation effects between the valence electrons and the $La^{1.6+}$ $O^{0.6-}$ ion core in some empirical parameter values. The present work gives the foundation of the LFT calculations. We, however, note that the configurations (assignments) given by the LFT[8] are different from the present ones. The LFT calculations can give assignments with hybridization and more detailed information from the LFT investigations is desired.

IV. CONCLUDING REMARKS

We have studied the electronic structures of LaO molecules using the RFCA four-component DHFR method, CASCI, MC-QDPT, and RASCI methods. We have learned that we can neglect the excitation from O $2p$ electrons when analyzing the experimental spectra of the lower excited states ($T_0 \leqq 4.2$ eV). This gives the foundation of the LFT calculations. The calculated excitation energies for LaO agree with the experimental values; the errors are within 0.6 eV. The spectroscopic constants have also been studied, and are in fairly good agreement with experiment, especially for the ground state.

ACKNOWLEDGMENTS

This study was partly supported by Grants-in-Aid for Scientific Research, Grant No. 16080216, to H.T. from the Ministry of Education, Culture, Sports, Science and Technology of Japan.

APPENDIX: THE LOWEST EXCITED STATE WITH AN O 2*p* HOLE BY RASCI

The small active-core MC-QDPT calculation gives the very lower excited states with an O $2p$ hole and these are considered as intruder-induced states. We therefore performed the RASCI calculation for $\Omega = 1/2 - 7/2$, which is free from the intruders. The excitation energies and dominant CSFs of LaO given by MC-QDPT with a large active-core and RASCI at $R = 3.45$ bohr are listed below, where the total energy of the first state of the large active-core calculation is $-8570.006\,457$ hartree, and the total energy of the first state of the RASCI calculation is $-8568.708\,486$ hartree. We find the calculated excitation energies (ΔE) according to the two calculations agree with the experiment. The lowest state with an O $2p$ hole is 5.15 eV above the ground state, as shown in the last row of the excitation energies and dominant CSFs of LaO, where the 17th and 18th spinors indicate O $2p$-like and La $6s$ spinors, respectively (see Table II). We may therefore disregard the contribution of the O $2p$ hole states to excited states lying below 5 eV.

		Expt.		MC-QDPT (large active core)			All-electron-RASCI (DIRAC)		
Desig.		T_0	Ω	ΔE (eV)	Ω	Dominant CSF	ΔE (eV)	Ω	Dominant CSF
X	$^2\Sigma^+$	0.000	1/2	0.000	1/2	|18|	0.000	1/2	|18|
A′	$^2\Delta$	0.926	3/2	0.989	3/2	|19|	1.350	3/2	|19|
A′	$^2\Delta$	1.013	5/2	1.091	5/2	|20|	1.395	5/2	|20|
A	$^2\Pi$	1.567	1/2	1.718	1/2	|21|	1.454	1/2	|21|
A	$^2\Pi$	1.673	3/2	1.843	3/2	|22|	1.535	3/2	|22|
B	$^2\Sigma^+$	2.212	1/2	2.520	1/2	|23|	2.229	1/2	|23|
C	$^2\Pi$	2.804	1/2	3.362	1/2	|25|	3.055	1/2	|24|
C	$^2\Pi$	2.832	3/2	3.404	3/2	|26|	3.151	3/2	|26|
D	$^2\Sigma^+$	3.157	1/2	3.635	1/2	|24|	3.142	1/2	|25|
F	$^2\Sigma^+$	3.554	1/2	4.068	1/2	|29|+|27|	3.468	1/2	|27|
				4.101	1/2	|27|−|29|	3.535	1/2	|29|
							5.150	1/2	$\|\cdots 15^2 16^2 17^1 18^2\|$

[1] S. H. Behere and P. L. Sardesai, Pramana **8**, 108 (1977).
[2] P. Carette, J. Mol. Spectrosc. **140**, 269 (1990).
[3] J. G. Bednorz and K. A. Müller, Z. Phys. **B64**, 189 (1986).
[4] A. Bernard, F. Taher, A. Topouzkhanian, and G. Wannous, Astron. Astrophys. Suppl. Ser. **139**, 163 (1999).
[5] K. P. Huber and G. Herzberg, *Molecular Spectra and Molecular Strucure. IV. Constants of Diatomic Molecules* (Van Nostrand, New York, 1979).
[6] R. A. Berg, L. Wharton, and W. Klemperer, J. Chem. Phys. **43**, 2416 (1965).
[7] W. Weltner, D. McLeod, and P. H. Kasai, J. Chem. Phys. **46**, 3172 (1967).
[8] L. A. Kaledin, J. E. McCord, and M. C. Heaven, J. Mol. Spectrosc. **158**, 40 (1993).
[9] J. Schamps, M. Bencheikh, J. C. Barthelat, and R. W. Field, J. Chem. Phys. **103**, 8004 (1995).
[10] M. Kotzian, N. Rösch, and M. C. Zerner, Theor. Chim. Acta **81**, 201 (1992).
[11] K. Schofield, J. Phys. Chem. A **110**, 6938 (2006).
[12] O. Matsuoka, J. Chem. Phys. **96**, 6773 (1992).
[13] Y. Watanabe and O. Matsuoka, J. Chem. Phys. **109**, 8182 (1998).
[14] T. Koga, H. Tatewaki, and O. Matsuoka, J. Chem. Phys. **117**, 7813 (2002).
[15] T. Koga, H. Tatewaki, and O. Matsuoka, J. Chem. Phys. **115**, 3561 (2001).
[16] S. Huzinaga, J. Andzelm, M. Klobukowski, E. Radzio-Andzelm, Y. Sakai, and H. Tatewaki, *Physical Science Data 16, Gaussian Basis Sets for Molecular Calculations* (Elsevier, New York, 1984).
[17] H. Moriyama, Y. Watanabe, H. Nakano, and H. Tatewaki, J. Phys. Chem. **112**, 2683 (2008).
[18] H. Moriyama, Y. Watanabe, H. Nakano, and H. Tatewaki, Int. J. Quantum Chem. **109**, 1898 (2009).
[19] H. Tatewaki, S. Yamamoto, Y. Watanabe, and H. Nakano, J. Chem. Phys. **128**, 214901 (2008).
[20] B. O. Roos, P. R. Taylor, and P. E. M. Siegbahn, Chem. Phys. **48**, 157 (1980).
[21] G. E. Brown and D. G. Ravenhall, Proc. R. Soc. London, Ser. A **208**, 552 (1951).
[22] J. Sucher, Phys. Rev. A **22**, 348 (1980).
[23] B. A. Hess, Phys. Rev. A **33**, 3742 (1986).
[24] M. Miyajima, Y. Watanabe, and H. Nakano, J. Chem. Phys. **124**, 044101 (2006).
[25] H. Nakano, J. Chem. Phys. **99**, 7983 (1993).
[26] R. S. Mulliken, J. Chem. Phys. **23**, 1833 (1955).
[27] H. Tatewaki and O. Matsuoka, J. Chem. Phys. **106**, 4558 (1997).
[28] U. Wahlgren, H. Moll, I. Grenthe, B. Schimmelpfennig, L. Maron, V. Vallet, and O. Gropen, J. Phys. Chem. A **103**, 8257 (1999).
[29] C. M. Marian, U. Wahlgren, O. Gropen, and P. Pyykkö, THEOCHEM **169**, 339 (1988).
[30] H. A. Witek, Y. K. Choe, and K. Hirao, J. Comput. Chem. **23**, 957 (2002).
[31] C. Camacho, H. A. Witek, and S. Yamamoto, J. Comput. Chem. **30**, 468 (2008).
[32] H. J. Aa. Jensen, T. Saue, L. Visscher *et al.*, DIRAC, a relativistic *ab initio* electronic structure program, Release DIRAC08.0, 2008; http://dirac.chem.sdu.dk.
[33] S. Yamamoto, H. Tatewaki, and T. Saue, J. Chem. Phys. **129**, 244505 (2008).